NASA/TM-20230010165 AIAA 2023–4470

Comparing the Electrical Modeling and Thermal Analysis Toolbox Simulation Data to Electrified Aircraft Propulsion Test Hardware Data

Mark E. Bell
HX5, LLC, Brook Park, Ohio

Santino J. Bianco and Jonathan S. Litt
Glenn Research Center, Cleveland, Ohio

July 2023

NASA STI Program . . . in Profile

Since its founding, NASA has been dedicated to the advancement of aeronautics and space science. The NASA Scientific and Technical Information (STI) Program plays a key part in helping NASA maintain this important role.

The NASA STI Program operates under the auspices of the Agency Chief Information Officer. It collects, organizes, provides for archiving, and disseminates NASA's STI. The NASA STI Program provides access to the NASA Technical Report Server—Registered (NTRS Reg) and NASA Technical Report Server—Public (NTRS) thus providing one of the largest collections of aeronautical and space science STI in the world. Results are published in both non-NASA channels and by NASA in the NASA STI Report Series, which includes the following report types:

- TECHNICAL PUBLICATION. Reports of completed research or a major significant phase of research that present the results of NASA programs and include extensive data or theoretical analysis. Includes compilations of significant scientific and technical data and information deemed to be of continuing reference value. NASA counter-part of peer-reviewed formal professional papers, but has less stringent limitations on manuscript length and extent of graphic presentations.

- TECHNICAL MEMORANDUM. Scientific and technical findings that are preliminary or of specialized interest, e.g., "quick-release" reports, working papers, and bibliographies that contain minimal annotation. Does not contain extensive analysis.

- CONTRACTOR REPORT. Scientific and technical findings by NASA-sponsored contractors and grantees.

- CONFERENCE PUBLICATION. Collected papers from scientific and technical conferences, symposia, seminars, or other meetings sponsored or co-sponsored by NASA.

- SPECIAL PUBLICATION. Scientific, technical, or historical information from NASA programs, projects, and missions, often concerned with subjects having substantial public interest.

- TECHNICAL TRANSLATION. English-language translations of foreign scientific and technical material pertinent to NASA's mission.

For more information about the NASA STI program, see the following:

- Access the NASA STI program home page at http://www.sti.nasa.gov

- E-mail your question to help@sti.nasa.gov

- Fax your question to the NASA STI Information Desk at 757-864-6500

- Telephone the NASA STI Information Desk at 757-864-9658

- Write to:
  NASA STI Program
  Mail Stop 148
  NASA Langley Research Center
  Hampton, VA 23681-2199

NASA/TM-20230010165 AIAA 2023–4470

Comparing the Electrical Modeling and Thermal Analysis Toolbox Simulation Data to Electrified Aircraft Propulsion Test Hardware Data

Mark E. Bell
HX5, LLC, Brook Park, Ohio

Santino J. Bianco and Jonathan S. Litt
Glenn Research Center, Cleveland, Ohio

Prepared for the
Aviation/Electrified Aircraft Technology Symposium (EATS)
cosponsored by AIAA and IEEE
San Diego, California, June 12–16, 2023

National Aeronautics and
Space Administration

Glenn Research Center
Cleveland, Ohio 44135

July 2023

Acknowledgments

The authors thank the Transformational Tools and Technologies (TTT) Project under NASA Aeronautics' Transformative Aeronautics Concepts Program (TACP) for funding this work.

This work was sponsored by the
Transformative Aeronautics Concepts Program.

Level of Review: This material has been technically reviewed by technical management.

This report is available in electronic form at https://www.sti.nasa.gov/ and https://ntrs.nasa.gov/

Comparing the Electrical Modeling and Thermal Analysis Toolbox Simulation Data to Electrified Aircraft Propulsion Test Hardware Data

Mark E. Bell
HX5, LLC
Brook Park, Ohio 44142

Santino J. Bianco and Jonathan S. Litt
National Aeronautics and Space Administration
Glenn Research Center
Cleveland, Ohio 44135

Abstract

A model using the Electrical Modeling and Thermal Analysis Toolbox (EMTAT), a National Aeronautics and Space Administration (NASA)-developed Simulink® model block library of electrical components, was developed to mirror the Hybrid Propulsion Emulation Rig (HyPER) hardware, a laboratory focused on Electrified Aircraft Propulsion (EAP) hardware tests. The goal of the model was to demonstrate the utility of the library by comparing the accuracy of the library models to the performance of real hardware, with the primary metrics being the simulation outputs matching physical test hardware data within 5 percent of full scale. The objective of this paper is to present the background, setup, testing and results of this comparison. It describes some of the adjustments that were necessary to match the system hardware, as well as next steps in verification and validation. The outputs of the model were compared to the results of several tests in HyPER, and in the process captured an additional torque loss that is still being analyzed for the root cause but has been confirmed in the hardware. Across all the test series, only one key model parameter was outside the target 5 percent full scale matching, and nearly 70 percent were within 1 percent.

1.0 Introduction

The Electrical Modeling and Thermal Analysis Toolbox (EMTAT) (Ref. 1) is a National Aeronautics and Space Administration (NASA)-developed modeling and simulation toolbox built on MATLAB® (Ref. 2) and Simulink® (Ref. 3). EMTAT contains blocks to represent electric machines (motors and generators), rectifiers, inverters, batteries, shafts, and loads, with the goal of facilitating system-level control design and analysis of electrified turbomachinery. This toolbox is a Simulink library, enabling users to add these blocks to new or existing simulation models. Electrified Aircraft Propulsion (EAP) is an area of research that investigates hybrid turbomachinery-electric or all-electric propulsion systems for electrical or electrified concept vehicles that are being proposed for traditional missions (Refs. 4 to 7). New types of vehicles for Urban Air Mobility (UAM) missions such as air taxi service are also under development (Ref. 8). These vehicle concepts require control design and operational concept analysis for their power and propulsion systems, as well as a dynamic simulation capability for the end-to-end system (Ref. 9). The models used to test these concepts must have high enough fidelity to capture the dominant system dynamics while being simple enough to speed up the calculations to enable real-time simulation outputs. The coupled nature of the propulsion and electrical systems in these concepts requires the model to have the capability for the electrical system to dynamically affect the performance of the turbomachinery,

and vice versa. EMTAT was developed at NASA Glenn Research Center (GRC) to meet this analysis need. EMTAT provides the capability to simulate the electrical components of these EAP systems at a timescale appropriate to capture the interaction with the turbomachinery. EMTAT is compatible with the NASA-developed Toolbox for the Modeling and Analysis of Thermodynamic Systems (T-MATS) software package (Ref. 10), which is used for modeling the dynamics of turbomachinery systems at the level of low frequency shaft dynamics, as well as the thermodynamics of said turbomachinery. These codes together enable models to be built of any of the various EAP architectures. The Hybrid Propulsion Emulation Rig (HyPER) laboratory at NASA GRC was developed to provide EAP hardware and hardware-in-the-loop control testing capability (Ref. 11). An EMTAT model of the HyPER laboratory test setup was developed to compare simulation models to real world hardware.

The rest of this paper is organized as follows. Section 2.0 describes the hardware and software utilized in the testing. Section 3.0 discusses some of the challenges in the testing and comparisons, and then shows the results of that testing. Finally, in Section 4.0, conclusions are drawn about the ability of the software to match real world hardware.

2.0 Tools and Methods

Most T-MATS simulations use a relatively large time step of ~15 ms, which captures engine dynamics at the level of low frequency shaft dynamics. Electronic components have much higher frequency dynamics, on the order of microseconds or nanoseconds, and typically reach steady state within a small fraction of the T-MATS time step. Steady state operation at each time step allows the electrical performance calculations to be simplified while still allowing general electrical system dynamics to be calculated. The electrical system component transients are captured as efficiency losses. EMTAT is not intended to replace small timestep, high fidelity electronic simulation tools such as the Simulation Program with Integrated Circuit Emphasis (SPICE) (Ref. 12), which is a global electronics industry standard public domain software for analyzing analog circuit behavior at nanosecond timescales (Ref. 13). Due to the very small timestep, however, SPICE runs significantly slower than real time; with simplified transient analysis, EMTAT model blocks can simulate faster than real time, making them more useful for testing control concepts. These blocks are equation-based, rather than dependent on a numeric solver, which increases the speed of simulation calculations. Point-by-point steady state operation of electrical components, while smoothing out the high-speed electrical transients, still demonstrates electrical system dynamics in operation at the turbomachinery time scale (Ref. 1). In addition, EMTAT model blocks can simulate realistic heat outputs and thermal rises, with associated performance impacts. EMTAT physics-based model blocks allow more specific performance tuning based on hardware specifications (Ref. 1). These physics-based component blocks were used to represent the physical hardware in HyPER.

HyPER is a reconfigurable EAP hardware and control laboratory located at the NASA Glenn Research Center at Lewis Field in Cleveland, Ohio (Ref. 11). The hardware components of HyPER are designed to be capable of dynamically representing a range of electrified turbomachinery. HyPER has two pairs of high-power electric machines, each pair directly connected by a shaft. This allows any given pair to operate in a motor-generator configuration, switching roles as needed. These motor-generator pairs can be used to simulate a gas turbine engine providing mechanical power to an electric machine to act as an electrical generator, an electric machine providing mechanical power to a gas turbine engine, and other configurations. The motor test table as configured for this testing is shown in Figure 1. The rig uses a

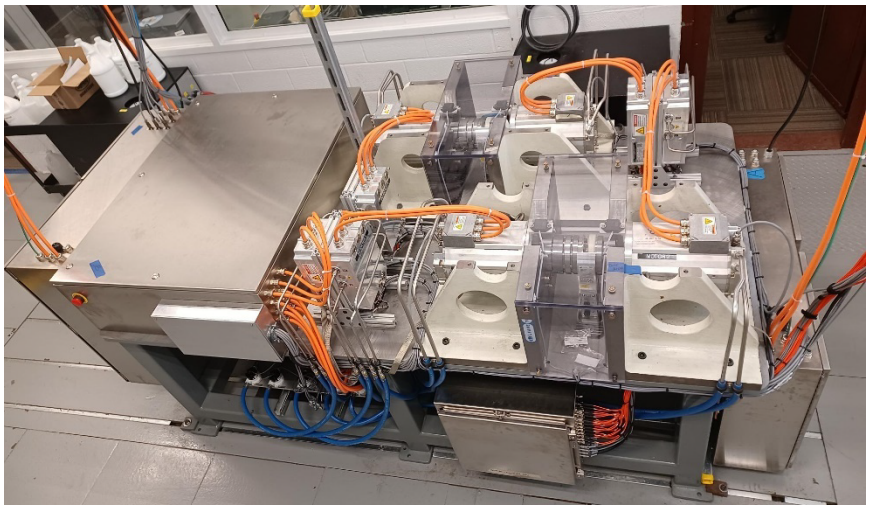

Figure 1.—HyPER laboratory motor test table.

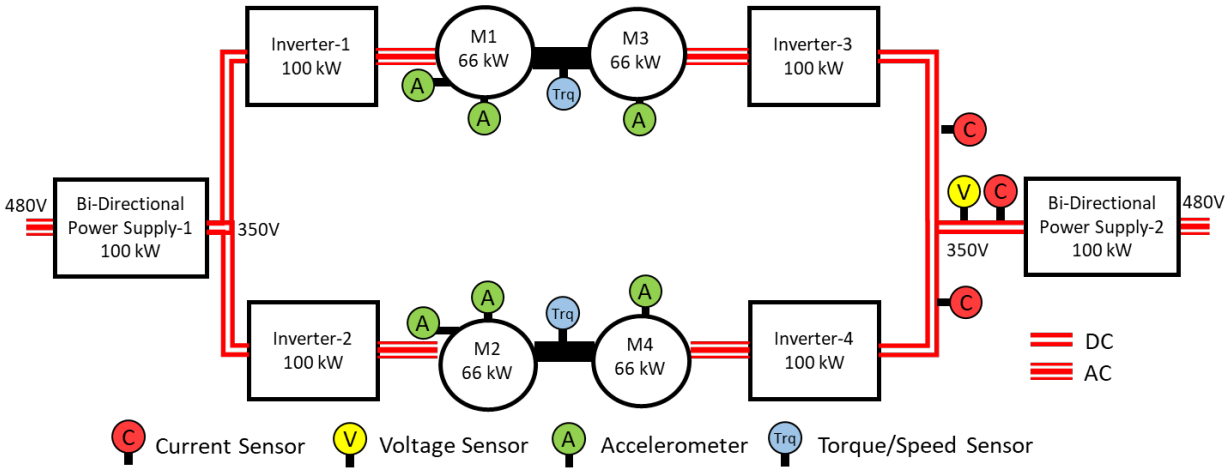

Figure 2.—HyPER configuration for electric machine checkout testing (Ref. 11).

variety of sensors and data recorders to collect data from the electric machines, motor controllers, cooling system, energy storage devices, and power supplies. The electric machines are Parker GVM210-150N6 Permanent Magnet Synchronous Motors (PMSMs), the inverters are Cascadia Motion Systems PM100DX motor controllers, and the bidirectional power supplies are NH Research (NHR) 9300-100 regenerative power supplies with a 100 kW limit. (The power system has the capability to regulate the direct current (DC) bus voltage using a super capacitor bank and a DC-DC voltage converter, but these were not used in this testing).

The HyPER configuration used to collect this test data is shown in Figure 2. This configuration was used to vary the speed and torques of the electric machines, both motoring and generating power. The two high power direct current (DC) bi-directional supplies are acting as power sources or power sinks as necessary. The two power supplies are connected to four bi-directional inverters (Inverter-1 through Inverter-4). The inverters are connected to one high power electric machine each (M1 through M4). The electric machines are grouped into two sets, M1–M3 (not used in these tests) and M2–M4, and each set of motors is mechanically connected with a shaft.

TABLE 1.—SIMULINK BLOCKS AND FUNCTIONS USED IN THE EMTAT HyPER MODEL

Block name	Library
Motor	EMTAT/Physics-based
Generator	EMTAT/Physics-based
Inverter	EMTAT/Physics-based
Rectifier	EMTAT/Physics-based
Resistor	EMTAT/Physics-based
Mechanical shaft	EMTAT/Power Flow
Integrator	Simulink/Continuous
PID controller	Simulink/Continuous
Memory	Simulink/Discrete
Gain	Simulink/Math operations
Product	Simulink/Math operations
Sum	Simulink/Math operations
Bus creator	Simulink/Signal routing
Bus selector	Simulink/Signal routing
From	Simulink/Signal routing
Goto	Simulink/Signal routing
Switch	Simulink/Signal routing
Display	Simulink/Sinks
Scope	Simulink/Sinks
Terminator	Simulink/Sinks
Constant	Simulink/Sources
Step	Simulink/Sources

The EMTAT model of HyPER emulated this setup with a variety of blocks from EMTAT (Ref. 1) as well as several standard Simulink functions, detailed in Table 1.

These components were laid out in a similar fashion to the physical arrangement of the machines in the HyPER laboratory, using datasheet information from the rig hardware to inform the performance of the digital models. The iDesign feature of EMTAT was used to calculate machine parameters that are not listed on the datasheets, such as magnetic flux and iron losses in the electric machines, or the internal diode and transistor losses in the inverters and rectifiers as a function of temperature (Ref. 1).

As is typical for EMTAT models, the voltage in the system is passed forward from one component to the next, while the current demands of the system are calculated at the end of the circuit and passed backwards from one component to the previous one. This allows the simultaneous calculation of each component's power, voltage, and current demands based on component efficiencies and physical operation. In this case, the speed of the shaft connecting the electric machines was used as a primary control reference. This was in addition to the power demand of the downstream power sink.

For these tests, HyPER was configured to run one half of an electric machine pair in a speed-controlled mode, with the controller adjusting the supplied torque to balance the load from the other half as necessary to maintain a constant speed. The other half of the pair was run in a torque-controlled mode, with the power supply acting as a load that adjusted as necessary to maintain the desired torque offtake, regardless of shaft speed.

The speed-controlled side of the EMTAT HyPER model is shown in Figure 3. The PID controller adjusts the torque demand on the speed-controlled electric machine to correct any deviations of the shaft speed from the setpoint. The EMTAT motor block calculates the required current to maintain that output torque based on physical component operating equations, given the voltage provided by the inverter and the current shaft speed. (The shaft block sums the total torques acting on it and adjusts its speed accordingly.) The inverter is given a fixed DC input voltage from the upstream power supply and

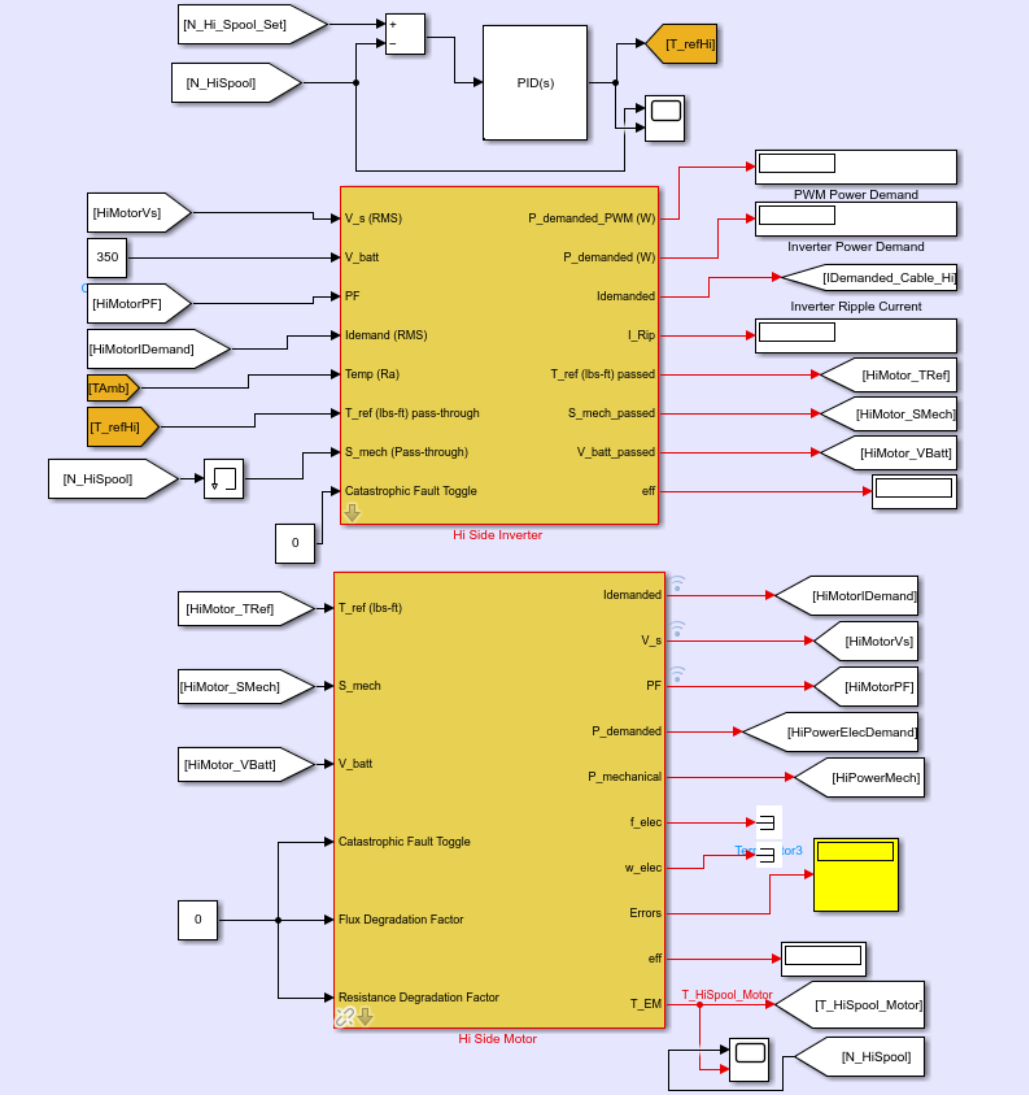

Figure 3.—EMTAT Model of the High Spool motor and speed controller side of the HyPER test setup.

provides the motor block an adjusted alternating current (AC) voltage for use in the motor calculations. The motor provides the inverter with a current demand, which is used to calculate the efficiencies and losses in the inverter. The inverter then provides a current demand to the power supply. (In these cases, it is assumed that the power supply can provide any required current to satisfy the system's power demands.) Since the electric machines can operate as either a motor or a generator, the selection of which EMTAT block to use to represent the electric machine was driven by the control mode. As a speed-controlled machine, whether it is adding torque to or extracting torque from the shaft to maintain a constant speed, the Motor block is designed to act primarily as a mechanical power source, and the motor torque output is determined by the PID.

The load controller is shown in Figure 4. A step function was used to delay the application of the torque load setpoint (allowing initial system transients to settle first). The torque controller PID then compared the torque setpoint to the measured torque the generator was applying to the shaft, adjusting the load resistance to increase or decrease said torque load to match. Once the resistance was set, the resistor calculated a current demand for the rectifier based on the DC bus voltage provided to it.

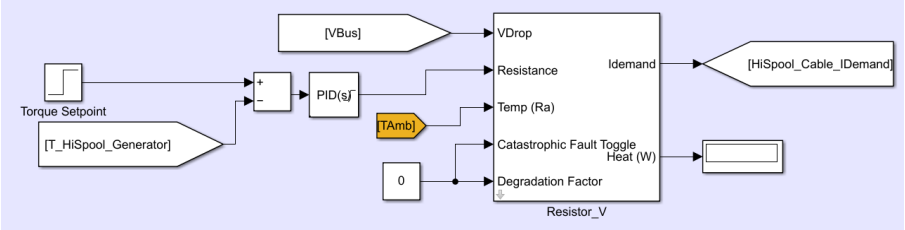

Figure 4.—EMTAT Model of the High Spool torque controller.

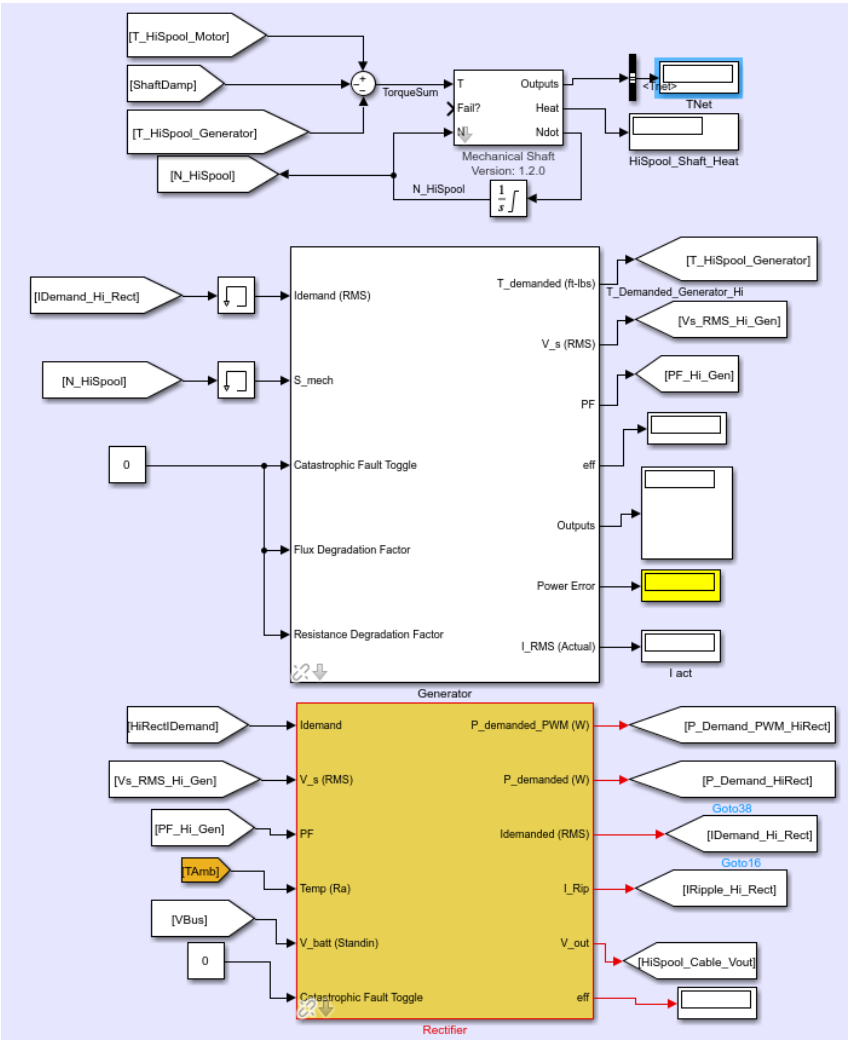

Figure 5.—EMTAT Model of the High Spool shaft and generator side of the HyPER test setup.

The torque-controlled side of the model is shown in Figure 5. The EMTAT generator block uses the shaft speed as an input to calculate the output AC voltage of the electric machine. The EMTAT rectifier block converts the AC voltage to a DC voltage and provides that to the load block as an DC bus voltage. The rectifier block then takes the calculated DC load current demand and converts it to an AC current demand on the generator block, which takes the AC current demand and converts it to a torque demand on the shaft block.

3.0 Results

The goal of the model was to demonstrate the utility of the library by comparing the EMTAT physics based model of the HyPER test setup to the actual hardware in the HyPER laboratory, with the primary metrics being the simulation outputs matching physical test hardware data within 5 percent of full scale. For these tests, the variables under comparison were the torque, speed, and current draw of each electric machine. The full-scale measurement ranges of the torque and current sensors (150 N-m and 500 A, respectively) were used as the reference for motor torque and current draw, while the speed error used the rated max speed of the machines (5,910 rpm).

The test data set that was used as a reference for the EMTAT model simulations encompassed a range of shaft speeds and torques. The goal was to have a broad representative sample of the operational range of the HyPER laboratory test hardware. To that end, the data sets were divided into several groupings. The primary grouping was based on shaft speed, with 1,000, 2,000, 3,000, and 4,000 rpm test data sets. The data was further grouped based on which electric machine was controlling the shaft speed through applied torque and which motor was controlling the torque extraction. Each data group contained a range of shaft torque extractions and additions, dwelling at each set point for approximately 30 s to allow the system to reach steady state. The torque extractions ranged from 130 N-m extracted to 130 N-m added. The convention used in the data sets was that negative values signified shaft power addition, while positive values signified shaft power extraction. When the controlling load for the torque-controlled side of the test hardware had a positive current demand, that electric machine was extracting power from the shaft, and thus had a positive value torque demand on the shaft. Conversely, a negative load created a negative current demand, which created a negative torque demand, and had the effect of adding torque to the shaft. A table of experiment set points is shown in Table 2.

Most of the lab hardware data was collected by the PM100DX inverters, which sample every 15 ms. In addition, the shaft speed/torque sensor (as seen in Figure 6) sampled at 50 μs. While maintaining a constant speed, the motors were swept through a range of torque setpoints, with the resulting torques and electrical bus currents recorded. In the raw data set, signal noise made it extremely challenging to determine the actual state of the hardware, as the point to point variations were quite high (DC Bus currents of ±2 A, shaft speeds of ±20 rpm, and torque variations of ±15 N-m). The first attempt to filter the lab data sets was to use 0.5 s windowed data point averages, which reduced but did not eliminate the noise and point-by-point variations. An example test data set is shown in Figure 6. The data represents a 3,000 revolutions per minute (rpm) test run of the M2–M4 motor pair, with M2 in a speed-controlled mode and M4 in a torque-controlled mode. This figure demonstrates the noise in the inverter torque calculations, DC bus current,[1] and the torque transducer, with no additional data filtering.[2]

TABLE 2.—TEST POINTS USED FOR COMPARISON

Speed, rpm	Speed mode	Torque mode	Shaft torque extraction, N-m									
1,000	M2	M4	–130	–90	–50	–30	–10	10	30	50	90	130
1,000	M4	M2	–130	–90	–50	–30	–10	10	30	50	90	130
2,000	M2	M4	–130	–90	–50	–30	–10	10	30	50	90	130
2,000	M4	M2	–130	–90	–50	–30	–10	10	30	50	90	130
3,000	M2	M4	–130	–90	–50	–30	–10	10	30	50	90	130
3,000	M4	M2	–130	–90	–50	–30	–10	10	30	50	90	130
4,000	M2	M4	–130	–90	–50	–30	–10	10	30	50	90	130
4,000	M4	M2	–130	–90	–50	–30	–10	10	30	50	90	130

[1]The DC bus current data, while noisy, tended to cluster around a few values at any given steady state condition.
[2]The torque transducer data was decimated by a factor of 300 to match the data rate of the inverters.

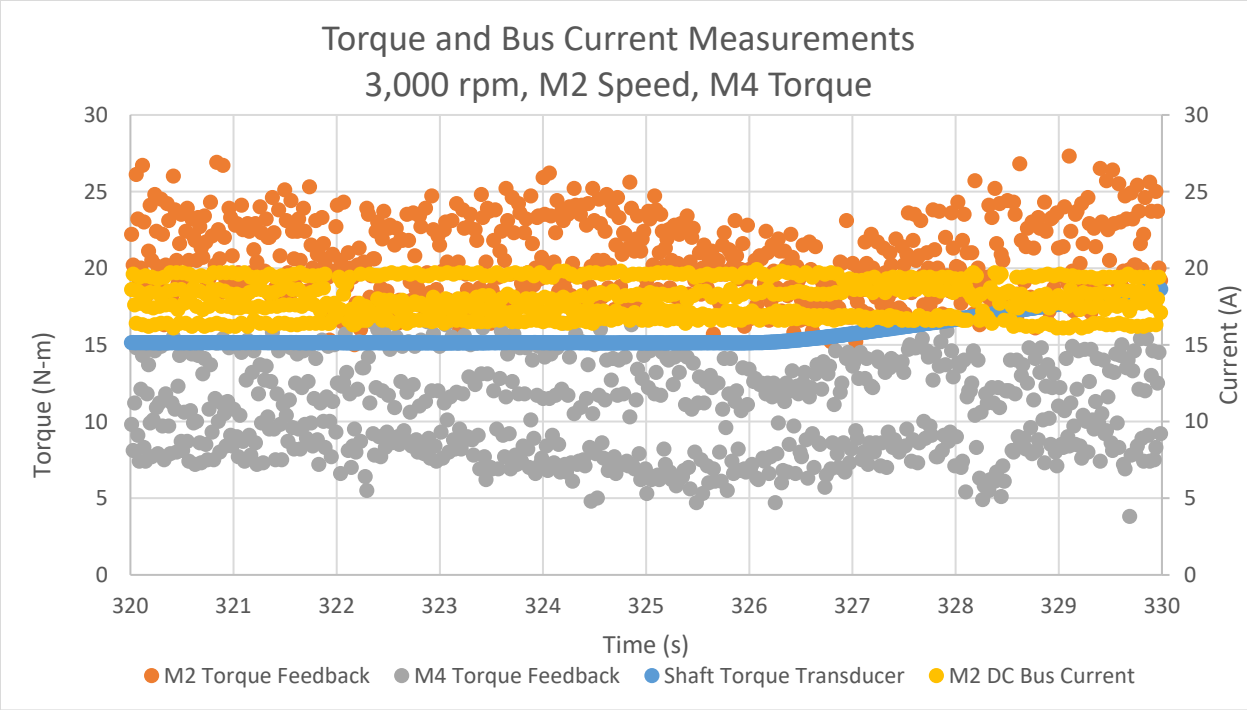

Figure 6.—Example test data comparing torque and current measurements. The discrete measurements represent the 15 ms sampling interval inherent to the PM100DX Inverters, which collected most of the electric machine data.

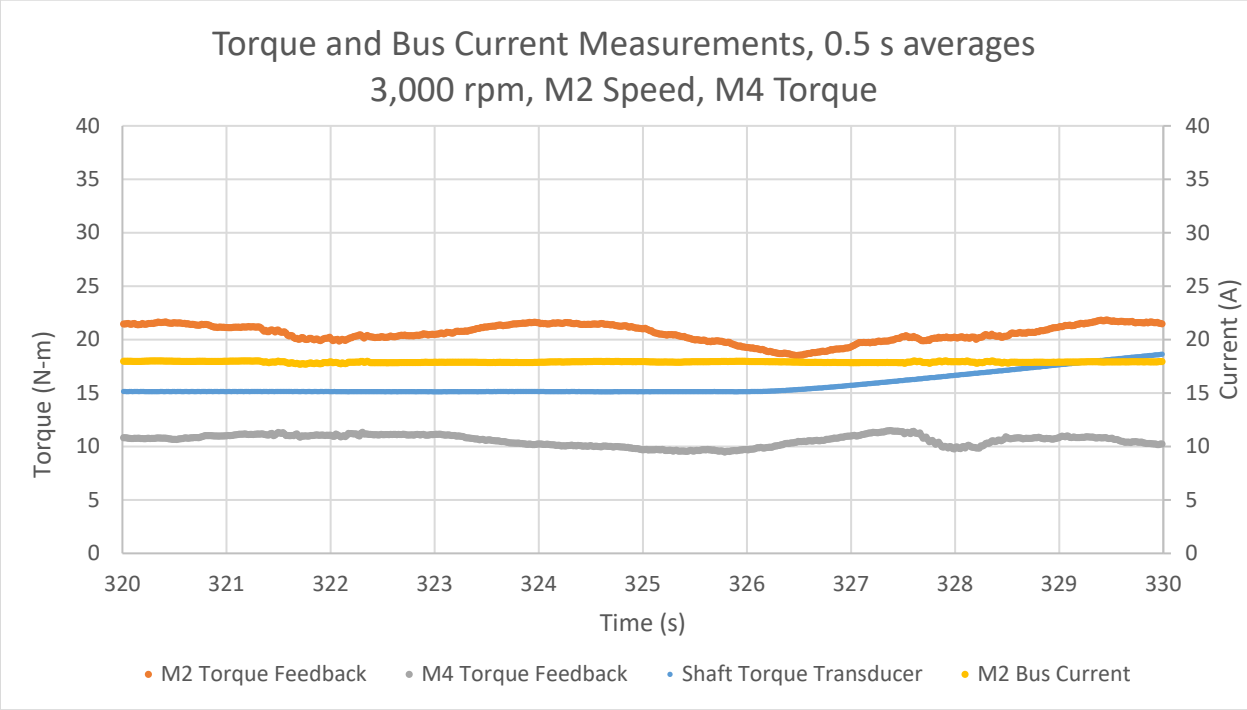

Figure 7.—Example test data comparing torque and current measurements, 0.5 s averages.

The same data set was then filtered by using 0.5 s data point averages, as seen in Figure 7. As this level of filtering still exhibited hardware data measurement variations over a given test point, the data was then filtered by averaging over the entire test point instead.

The EMTAT control inputs were the shaft torque extraction and the shaft speed, and each filtered steady state test point was used as inputs for the simulation model. As the simulations were initially conducted, the outputs were largely not within the 5 percent spec called out as a goal. The primary issues appeared to be the torque applied to the shaft by the motor block and the current demanded by the motor block on the upstream power supplies. The issue was more pronounced as the shaft torque demands increased. An example of the initial comparison to test data is shown in Table 3.

To attempt to understand the root cause of the differences,[3] the shaft torque/speed sensor (a high sampling rate torque (HST) transducer) data was filtered and compared to the electric machine torque data. A sample data set is shown in Figure 8, showing the calculated difference between the electric machine torque feedback and the HST transducer data. This torque difference was characterized as a torque offset on the shaft, and in Figure 8 the calculated offset is plotted on the secondary axis for clarity.

TABLE 3.—DIFFERENCE BETWEEN INITIAL EMTAT OUTPUTS AND HYPER IN PERCENT FULL SCALE FOR THE 3,000 rpm TEST RUN

	Shaft torque extraction, N-m									
Percent difference full scale	–130	–90	–50	–30	–10	10	30	50	90	130
M2 rpm	0.82	–0.02	–0.02	–0.02	–0.02	–0.01	–0.04	–0.01	–0.01	–0.02
M2 bus current	–6.10	–5.21	–2.59	–2.12	–1.58	1.66	1.38	0.79	–2.01	–2.54
M2 torque	1.71	–8.81	–8.88	–7.28	–6.24	7.44	6.13	5.73	7.67	17.81
M4 rpm	–0.83	0.02	0.02	0.02	0.01	–0.01	0.00	0.01	0.03	0.00
M4 bus current	9.61	6.87	3.85	2.26	0.77	0.80	2.41	3.88	6.60	8.86
M4 torque	0.11	–0.77	0.90	0.03	–0.49	0.14	0.94	–0.99	0.71	1.73

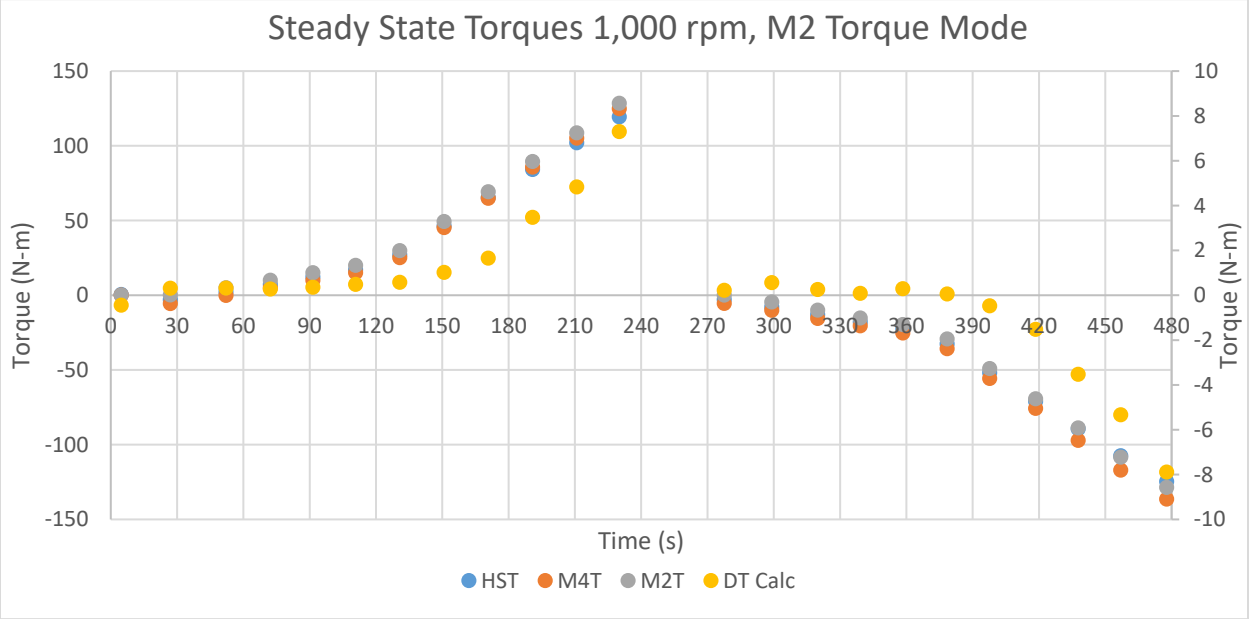

Figure 8.—Test data set comparing electric machine 2 and electric machine 4 feedback torque (M2T and M4T, respectively) to the High Sampling rate Torque (HST) transducer during a 1,000 rpm test, and the resulting torque offset calculations plotted on the secondary vertical axis for clarity.

[3]In full scale turbomachinery systems, shaft damping torques are relatively much smaller compared to the torques being applied and may be negligible. In this study, it was significant enough that neglecting it in the simulation led to many instances of missing the target accuracy goal.

Other data sets had similar relationships between the torque offsets and shaft torque extraction. Shaft damping torque, which is understood to be a function of shaft speed, did not have enough data to determine the exact relationship to the test rig shaft speed. All the motor testing was conducted by varying torque additions and extractions at four fixed speeds, so each speed comparison only really had four points to compare. Further testing may look at the effects of fixed system torque setpoints while changing speed over time to ascertain if there are more speed effects than can be determined from more varied speed data. The inverter torque measurements are a function of measured current and electric machine parameters and were monotonic relative to the commanded and transducer measured torques.[4]

For the simulation, the damping torque was determined experimentally at each test point. This damping torque did not match the measured torque offsets, either between the two inverter torque measurements or the inverters compared to the HST transducer measurements. This damping torque was mostly contained in the range of ±10 N-m, depending on the test point. The experimentally determined model damping torques were not monotonic relative to either motor torques or shaft speeds and are listed in Table 4 to Table 7.

TABLE 4.—DIFFERENCE BETWEEN EMTAT OUTPUTS AND HYPER RESULTS IN PERCENT FULL SCALE FOR THE 1,000 rpm TEST RUN

	Shaft torque extraction, N-m									
Percent difference full scale	–130	–90	–50	–30	–10	10	30	50	90	130
M2 rpm	–0.06	0.00	–0.03	–0.04	–0.05	–0.05	–0.05	–0.02	–0.04	–0.07
M2 bus current	–0.53	–0.38	–0.16	–0.10	–0.11	–0.31	–0.36	–0.65	–1.59	–2.75
M2 torque	–0.78	0.07	–0.19	0.28	0.00	–0.10	0.08	0.45	0.32	–0.97
M4 rpm	0.06	0.03	0.06	0.04	0.03	0.06	0.07	0.04	0.03	0.05
M4 bus current	1.54	0.93	0.52	0.33	0.06	0.11	0.50	0.55	0.92	0.97
M4 torque	–0.10	0.09	–0.23	0.11	0.12	–0.15	–0.18	–0.10	0.14	0.00
Damping torque (N-m)	7	7	5	3	5	5	3.5	2	4	5.5

TABLE 5.—DIFFERENCE BETWEEN EMTAT OUTPUTS AND HYPER RESULTS IN PERCENT FULL SCALE FOR THE 2,000 rpm TEST RUN

	Shaft torque extraction, N-m									
Percent difference full scale	–130	–90	–50	–30	–10	10	30	50	90	130
M2 rpm	0.08	–0.01	–0.06	–0.01	–0.01	–0.08	–0.07	–0.02	–0.04	0.10
M2 bus current	–0.66	0.03	–0.48	–0.33	–0.34	–0.26	–0.64	–0.63	–2.15	–3.41
M2 torque	0.44	0.05	–0.08	–0.22	0.19	0.24	0.67	0.38	0.08	–0.12
M4 rpm	0.06	0.00	–0.01	0.05	0.00	–0.05	–0.04	0.00	0.09	0.08
M4 bus current	2.72	1.72	0.99	0.55	0.38	0.20	0.85	1.31	1.31	1.64
M4 torque	0.01	0.00	0.01	0.01	–0.03	0.01	0.03	–0.15	0.08	–0.19
Damping torque (N-m)	10.5	12	6	6	4.5	5.25	7	5	5	5

[4]The inverters use current sensors with an accuracy of 1 percent and each inverter is factory calibrated, although motor parameter inputs would need to be comparably precise to maintain that accuracy. 5 to 10 percent unit to unit torque calculation variation may be seen, depending on machine parameter accuracy. (Correspondence with Cascadia Sr. Applications Engineer T. Gintz, 4/13/2023)

TABLE 6.—DIFFERENCE BETWEEN EMTAT OUTPUTS AND HYPER RESULTS IN PERCENT FULL SCALE FOR THE 3,000 rpm TEST RUN

	Shaft torque extraction, N-m									
Percent difference full scale	–130	–90	–50	–30	–10	10	30	50	90	130
M2 rpm	–0.02	–0.02	–0.02	–0.02	–0.02	–0.02	–0.04	–0.01	–0.01	–0.02
M2 bus current	–1.58	–0.27	–0.11	–0.20	–0.36	–0.36	–0.53	–0.71	–2.52	–4.06
M2 torque	–0.08	–0.05	0.06	0.94	–0.44	–0.44	0.08	0.19	–0.30	–0.31
M4 rpm	0.00	0.02	0.02	0.02	0.01	0.01	0.00	0.01	0.03	0.00
M4 bus current	3.71	2.63	1.71	0.89	0.25	0.25	1.17	1.43	2.58	3.12
M4 torque	0.11	0.00	0.13	0.03	–0.10	–0.10	0.17	–0.22	–0.06	0.19
Damping torque (N-m)	8.75	11.25	8.5	8.5	8.5	7	7	5	9	9

TABLE 7.—DIFFERENCE BETWEEN EMTAT OUTPUTS AND HYPER RESULTS IN PERCENT FULL SCALE FOR THE 4,000 rpm TEST

	Shaft torque extraction, N-m									
Percent difference full scale	–130	–90	–50	–30	–10	10	30	50	90	130
M2 rpm	0.01	–0.16	–0.01	0.10	–0.08	–0.13	–0.12	–0.19	0.11	0.07
M2 bus current	–1.45	–1.48	–0.36	0.16	–0.02	–0.40	0.13	–0.17	–2.48	–4.87
M2 torque	0.01	0.15	0.10	–0.07	0.04	–0.01	0.12	0.20	–0.11	–0.06
M4 rpm	–0.06	0.04	0.08	–0.11	–0.06	0.18	0.17	–0.12	–0.10	0.20
M4 bus current	5.40	3.63	1.97	0.87	0.35	–0.12	1.24	2.29	3.77	1.94
M4 torque	0.25	0.03	–0.06	–0.01	0.03	–0.04	0.07	0.08	–0.03	0.01
Damping torque (N-m)	7	8	8.25	9.25	7.75	3.25	1	4.5	8.5	3

Steady state simulation data was compared to steady state test data at various points throughout the operating envelope of the motors. Results from comparing the EMTAT simulation outputs to the recorded HyPER results for the 4 speed setpoints (1,000, 2,000, 3,000, and 4,000 rpm) are presented in Table 4 to Table 7. Across all the test series, only one key model parameter was outside the target 5 percent full scale spec, and nearly 70 percent were within 1 percent.

4.0 Conclusion

EMTAT provides a simple-to-use electrical modeling and simulation tool that facilitates control design, analysis, evaluation, and virtual testing of electrified aircraft propulsion concepts. The results of the testing show that the EMTAT Physics Based library blocks can match or nearly match real hardware in a test environment over a range of steady state speeds and power, with the model moving smoothly from positive to negative power on any given device. Only one point was outside the specified tolerance range of 5 percent, and 70 percent of the comparison points were within 1 percent matching, which exceeded our expectations. Going forward, more analysis is planned to understand other differences in the data matching, particularly in the DC bus current calculations, as well as to match the hardware's electrical system dynamics at the turbomachinery timescale. Additionally, more varied speed data can be collected to determine the relationship of the test rig shaft speed to the shaft damping torque. Finally, clarification of the relationship of the model damping torque to hardware damping torques would improve the functionality of the model as it applies to other hardware designs. It additionally demonstrated the utility of the program for detecting test system abnormalities.

References

1. Bell, M., and Litt, J., “An Electrical Modeling and Thermal Analysis Toolbox for Electrified Aircraft Propulsion Simulation,” AIAA-2020-3676, AIAA Propulsion and Energy Forum, August 2020, virtual.
2. MATLAB, Software Package, Ver. 9.11 (R2021b), The MathWorks, Inc., Natick, MA, 2021.
3. Simulink, Software Package, Ver. 10.4 (R2021b), The MathWorks, Inc., Natick, MA, 2021.
4. Bradley, M.K., and Droney, C.K., “Subsonic Ultra Green Aircraft Research: Phase II—Volume II—Hybrid Electric Exploration,” NASA/CR—2015-218704, 2015.
5. Schiltgen, B.T., Freeman, J.L., and Hall, D.W., “Aeropropulsive Interaction and Thermal System Integration within the ECO-150: A Turboelectric Distributed Propulsion Airliner with Conventional Electric Machines,” AIAA Aviation Technology, Integration and Operations Conference, AIAA-2016-4064, AIAA, Reston, VA, 2016.
6. Welstead, J., and Felder, J.L., “Conceptual Design of a Single-Aisle Turboelectric Commercial Transport with Fuselage Boundary Layer Ingestion,” 54th AIAA Aerospace Sciences Meeting, AIAA-2016-1027, Reston, VA, 2016.
7. Felder, J.L., Brown, G.V., and Kim, H.D., “Turboelectric Distributed Propulsion in a Hybrid Wing Body Aircraft,” 20th International Society for Airbreathing Engines, ISABE-2011-1340, Gothenburg; Sweden, 2011.
8. Silva, C., Johnson, W., Antcliff, K.R., Patterson, M.D., “VTOL Urban Air Mobility Concept Vehicles for Technology Development,” AIAA-2018-3847, AIAA AVIATION Forum, June 25–29, 2018, Atlanta, Georgia.
9. Bianco, S.J., Chevalier, C.T., Litt, J.S., Smith, J.K., Chapman, J.W., Kratz, J.L., “Revolutionary Vertical Lift Technology (RVLT) Side-by-Side Hybrid Concept Vehicle Powertrain Dynamic Model,” GT2021-59375, Turbo Expo 2021, June 7–11, 2021.
10. Chapman, J.W., Lavelle, T.M., May, R.D., Litt, J.S., Guo, T.H., “Propulsion System Simulation Using the Toolbox for the Modeling and Analysis of Thermodynamic Systems (T-MATS),” AIAA 2014-3929, 50th AIAA/ASME/SAE/ASEE Joint Propulsion Conference, Cleveland, OH, July 28–30, 2014.
11. Buescher, H.E., Culley, D.E., Bianco, S.J., Connolly, J.W., Dimston, A.E., Saus, J.R., Theman, C.J., Horning, M.A., and Purpera, N.C. “Hybrid-Electric Aero-Propulsion Controls Testbed: Overview and Capability,” AIAA 2023-0671. AIAA SCITECH 2023 Forum. January 2023.
12. Nagel, N.W., and Pederson, D.O. “Simulation Program with Integrated Circuit Emphasis (SPICE),” Midwest Symposium on Circuit Theory, Ontario, Canada, April 1973 www.eecs.berkeley.edu/Pubs/TechRpts/1973/ERL-382.pdf
13. Vladimirescu, A. “SPICE: The third decade,” Proceedings on Bipolar Circuits and Technology Meeting. September 1990. doi:10.1109/BIPOL.1990.171136.